AD 409 487

CARNEGIE INSTITUTE OF TECHNOLOGY

PITTSBURGH 13, PENNSYLVANIA

SOME MECHANICAL PROPERTIES OF AUSTENITIC STAINLESS STEEL SINGLE CRYSTALS

27 May 1963

CONTRACT Nonr 760 (14) NR 036-029

Metallurgy Branch

OFFICE OF NAVAL RESEARCH

Washington 25, D. C.

SOME MECHANICAL PROPERTIES OF AUSTENITIC STAINLESS STEEL SINGLE CRYSTALS

by

G. Meyrick[#] and H. W. Paxton[*]

[#] Formerly Assistant Professor of Metallurgical Engineering, Carnegie Institute of Technology, now at N.P.L., Teddington, England.

[*] Professor of Metallurgical Engineering, Carnegie Institute of Technology.

ABSTRACT

Observations on the tensile deformation of single crystals of austenitic stainless steels as a function of composition, orientation and temperature are described and compared with relevant data for other alloys. Crystals free from second phases show sharp yield points followed by Lüders' extensions of up to 20%. The critical resolved shear stress is strongly temperature dependent increasing fourfold between 423°K and 77°K. A temperature independent low rate of hardening follows the Lüders' extension and is frequently associated with overshoot. Unlike pure metals where profuse cross-slip usually occurs at the end of linear hardening, this stage is terminated either by cross-slip or by slip on the conjugate system; the particular mode apparently depending upon initial orientation and composition.

The presence of δ-ferrite or martensite has a profound effect upon the magnitude of the yield stress and the shape of the stress-strain curve.

INTRODUCTION

In experiments on transgranular stress corrosion cracking of austenitic stainless steels in boiling magnesium chloride, several workers[1,2] have shown that increasing amounts of nickel tend to reduce the probability of specimen failure. Reed and Paxton[3] have observed in single crystals that the macroscopic crack plane changes as the nickel content is increased. For 18% Cr - 8% Ni, the crack plane is sensibly perpendicular to the applied tensile stress; for 20% Cr - 20% Ni the crack plane is $\{100\}$. The average crack propagation speed is much lower in the 20% Ni crystals.

Furthermore, the possible importance of stacking fault energy in nucleation and growth of cracks has been suggested by a number of workers. While the general effect of variations in stacking fault energy appears to be quite well correlated with observed variations in cracking characteristics, each of the theories assigns rather different detailed reasons for these effects.

Because the stacking fault energy of austenitic steels is believed to be increased with increasing nickel

content, and because some theories of transgranular cracking postulate a mechanical stage in the crack propagation (rather than relying entirely on electrochemical solution), it appeared to be of some interest to investigate the mechanical properties of a series of different compositions of austenite single crystals. These experiments were considered of intrinsic value in view of the relative scarcity of such data on face centred cubic alloys. This paper gives the results of some experiments carried out with this aim in mind, and suggests various other experiments which may be helpful in future studies. Comparisons with experiments on other face-centred cubic alloy crystals are made where possible to see how well the general pattern of behaviour is understood.

EXPERIMENTAL PROCEDURE

The alloys used in this investigation were vacuum melted heats of nominally 20% Cr - 20% Ni - 60% Fe, 20%Cr - 16% Ni - 64% Fe and 20% Cr - 12% Ni - 68% Fe.* Analyses of the material are given in Table 1.

*These alloys were obtained through the courtesy of the Allegheny Ludlum Steel Corporation Research Laboratory in Pennsylvania.

TABLE 1

CHEMICAL ANALYSES OF THE STARTING MATERIALS

Nominal Composition	Cr	Ni	C	N_2
20% Cr - 20% Ni	20.2	19.87	0.017	
20% Cr - 16% Ni	20.02	16.04	0.0041	.0024
20% Cr - 12% Ni	19.82	12.14	.0014	.0048

Other minor impurities included Mn, P, S and Si.

Single crystals, 9 cms long and 15 cm^3 in volume, were grown from the melt using a technique similar to that described by Leggett et al.[4] The molten alloy, contained in a horizontal recrystallized alumina boat under purified argon, was slowly withdrawn from the hot zone of a glo-bar furnace. For this purpose the boat was carried inside an alumina tube which was suspended from a trolley free to move along a horizontal monorail.

Alloys containing 20% Ni and 16% Ni were entirely austenitic and single crystals of these compositions were grown with reasonable ease. On solidification, the 12% Ni alloy contained both austenite and delta ferrite. However monocrystals were obtained successfully although the fraction of successful attempts was lower. These crystals consisted of a continuous austenitic matrix in which particles of ferrite were embedded. After growth the crystals were annealed for several days at 1200°C in purified hydrogen to reduce the ferrite content and local composition variations due to segregation. Variations along the crystals were not examined but are quite small according to Leggett et al.[4]

Tensile specimens, of rectangular (close to square) cross section, were prepared from the single crystal ingots by a series of sectioning and polishing operations during which the samples were frequently chemically etched

and care taken to avoid excessive damage. Finally the crystals were deeply electropolished, annealed in hydrogen at 1100°C for 6 hrs, slowly cooled and then silver-soldered into stainless steel grips. A gauge length* of about 1.8 inches, which gave a length to thickness ratio of about 25 : 1, was employed. The axial orientations were determined by means of back-reflection X-ray photography. Tensile tests were carried out on a standard Instron machine, at a strain rate of about $1.8 \times 10^{-4} sec^{-1}$ at temperatures of 77°K, 195°K, 293°K and 423°K. The first two temperatures were attained by immersing the samples in suitable constant temperature baths while for the last the specimen was surrounded by a resistance wound furnace.

Some tests were frequently interrupted and slip patterns corresponding to various amounts of strain examined by optical microscopy. These observations were supplemented in some cases by measurements of the changes in axial orientation which occurred during deformation.

*With the technique employed it was not possible to produce samples of identical sizes. Individual gauge lengths were within 10% of 1.8 inches and the cross sectional areas were within 20% of 5×10^{-3} square inches. The nominal strain rate thus does not vary significantly.

For this purpose an X-ray source and camera were mounted on the crosshead of the testing machine. At suitable intervals tests were stopped and photographs taken while the specimen was in situ; axiality was maintained by retaining a small load. To reduce errors introduced by changing the film, several exposures, each for a different strain, were frequently made on the same film. This was impracticable at large strains since decreased numbers of spots and the presence of asterism caused difficulty in the interpretation of the photographs. In conjunction with these measurements, the planes associated with the observed slip traces were identified by the application of stereographic projection techniques to optical micrographs of the slip patterns.

RESULTS

It is convenient to present the general observations made on each alloy separately and finally compare them as a function of composition and temperature.

20% Cr - 20% Ni - 60% Fe

Specimens of this composition exhibited a drop in load at yield, followed by up to 20% elongation at constant load. The amount of this elongation was slightly temperature dependent, increasing with decrease in temperature. This

behaviour was associated with the initiation and propagation of a Lüders' band along the gauge length. Normally only one band was formed but occasionally two, one at each grip, occurred. The strain within the Lüders' band, at any instant, was the same as the total strain in the gauge length at the completion of the passage of the band, (i.e. the Lüders' strain), as is normal for this type of deformation. Samples unloaded before the Lüders' extension was completed showed no change in flow stress when reloaded immediately or after a week at room temperature. However, the yield point effect could be recovered after an anneal in vacuo at 350°C for 24 hours. As a quick check on the effect of interstitials, a few crystals were annealed at 1200°C for 30 hours in nitrogen or in vacuum prior to testing, to change the amount of nitrogen in solution. No noticeable differences in the yield behaviour were noted; analyses for nitrogen were not performed.

The Lüders' band was comprised of long parallel slip traces, the spacing of which was uniform within the band but increased gradually across its front. Outside the band there was usually no evidence of slip, especially for low temperature deformation, although a few widely spaced slip bands were sometimes seen. These may have been due to some slight non-axiality during initial loading. The lattice rotation within the band agreed closely with that calculated

by assuming slip to occur on the system upon which the resolved shear stress was a maximum.

Those specimens which were extended to failure may be divided into two groups, according to orientation. This is illustrated in Fig. 1 in which the initial orientations of the tensile axes are plotted on a stereographic projection. Included on this diagram are examples of orientation changes to be described below. Samples of group B were of identical orientations within one degree while there was rather more scatter for those of group A.

All the specimens behaved similarly in the initial stages of elongation but there were some differences between the two groups in the later stages of deformation. Fig. 2 depicts the load-extension curves obtained from a sample of each group at room temperature.

For all specimens linear work hardening began when the Lüders' band had filled the gauge length. In the case of group A, slip continued on the primary slip planes and, in addition, short traces of slip on the cross-plane appeared (Fig. 3). These increased in number as deformation proceeded. Meanwhile the rotation of the tensile axis proceeded, within experimental error, along the great circle joining the initial orientation, A, (Fig. 1) and the pole of the $(1\bar{1}0)$ planes. As the symmetry line was approached (S)

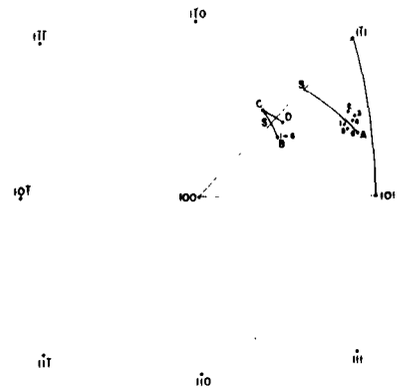

FIG. 1. Orientation of crystal sets A and B (20% Cr - 20% Ni).

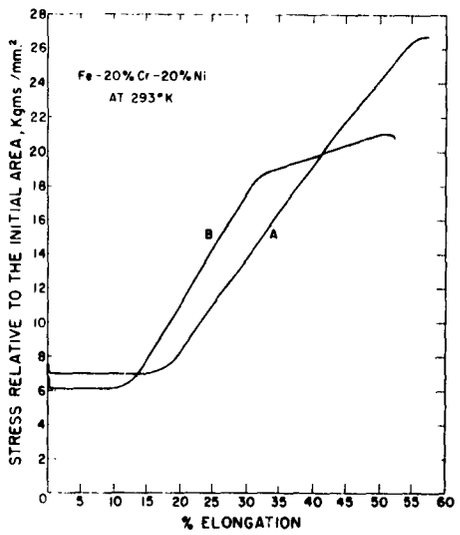

FIG. 2. Load-extension curves for samples from sets A and B at 293 °K.

a severe reduction in the number of spots, in addition to asterism, prevented further orientations being reliably determined. The linear stage was terminated by a gradual reduction in the rate of hardening during which considerable cross slip was evident. Finally necking associated with localized long-range slip on the conjugate $(1\bar{1}\bar{1})$ planes set in followed rapidly by failure.

Upon completion of the Lüders' extension in group B specimens, the tensile axis lay close to the symmetry line. During linear hardening slip continued on the primary planes, while a few short traces due to slip upon the cross-planes $(11\bar{1})$ appeared, as shown in Fig. 4. These were far less prolific than those observed for samples of group A and did not increase in number particularly, as deformation proceeded. This stage was associated with "overshoot" where the rotation of the axial orientation towards the $1\bar{1}0$ direction continued until it reached C, at which point the orientation agreed closely with that calculated assuming single slip on the (111) $[1\bar{1}0]$ system. Instead of giving way to a region of gradual reduction in the rate of hardening, as observed in group A, the linear stage was followed by a second linear region of smaller slope. This stage corresponded to the appearance of long slip traces, due to slip on the conjugate $(1\bar{1}\bar{1})$ planes (Fig. 5), which continued to be formed

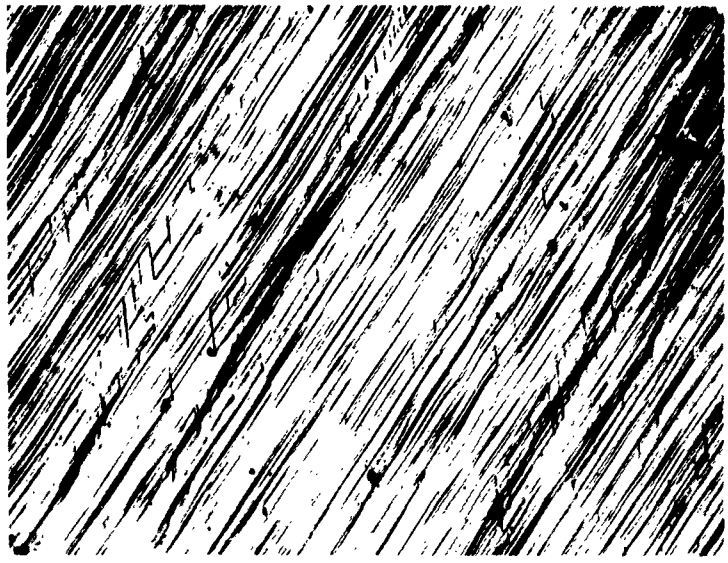

FIG. 3 Specimen from set A strained at 298°K
X290 ε = 30% Tensile axis $\longleftrightarrow$

FIG. 4 Specimen from set B strained at 298°K
X90 ε = 20% Tensile axis $\longleftrightarrow$

until they occupied the whole gauge length. Little, if any, cross slip was detected by optical microscopy. In keeping with these observations the orientation changed so that the axis rotated back across the symmetry line to D. Again the rotation C → D agreed well with that calculated assuming single slip upon the system $(1\bar{1}\bar{1})\ [101]$ although this was to some extent fortuitous since the final orientation determination was subject to an error of several degrees due to scarcity of spots and asterism. Occasional traces of slip on the $(1\bar{1}1)$ planes were observed during the second linear stage; eventually pronounced localized slip on these planes caused necking prior to failure.

It is recognised that observations of slip traces by optical microscopy afford a minimum description of the slip activity, particularly as regards the crystal interior. Since reasonable consistency among the observations described and calculated orientation changes was obtained, resolved shear stress - shear strain curves were computed using the classical relations of Schmid and Boas[5].* Examples of these are presented in Figs. 6 and 7. The discontinuities on some curves

*There is some uncertainty as to how this resolution should be performed during the Luder's extension where slip is occurring within a small region at the front of the moving band. In the curves shown in this article this stage is represented by a line of constant stress, that of the lower yield point, which is finally smoothly curved to meet the work hardening curve. Formally, since the part of the material behind the Luder's front is at a higher shear stress, two lines parallel to the strain axis represent the limits of stress in the crystal. Since this complicates the graphs and adds little to our understanding for these purposes, this refinement has been omitted.

correspond to points where the resolution was made on the conjugate slip system for those specimens in which a second linear region occurred.

20% Cr - 16% Ni - 64% Fe

The general characteristics of the deformation of this alloy, at the three highest temperatures employed, were very similar to those described for the previous composition. In a few samples second linear hardening regions were again observed although they were shorter than those previously described. Slip bands corresponding to slip upon the conjugate planes were formed during this stage but did not cover the whole gauge length. Instead, when about half the gauge length was occupied, necking and subsequent failure took place.

Examples of the resolved stress-strain curves are shown in Fig. 8 while the specimen orientations are given in Fig. 9 which also depicts an observed axial rotation indicating the occurrence of overshoot.

Tests conducted at 77°K were complicated by the formation of martensite which was detected both by microscopic observations and by characteristic discontinuous load oscillations; the latter were often accompanied by audible clicks. Martensite was not observed in samples cooled to

FIG. 5 Specimen from set B strained at 293°K
X90 ε = 35% Tensile axis ≈ ⟷

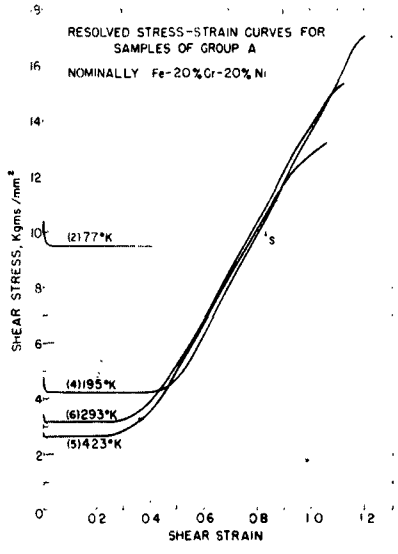

FIG. 6 Specimens from set A extended at various temperatures. S marks symmetry line.

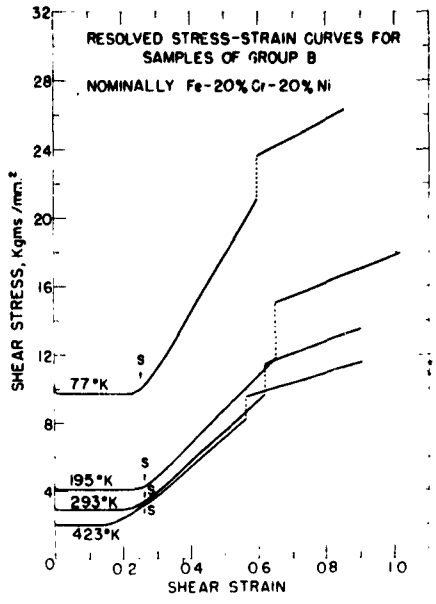

FIG. 7. Specimens from set B extended at various temperatures. S marks symmetry line.

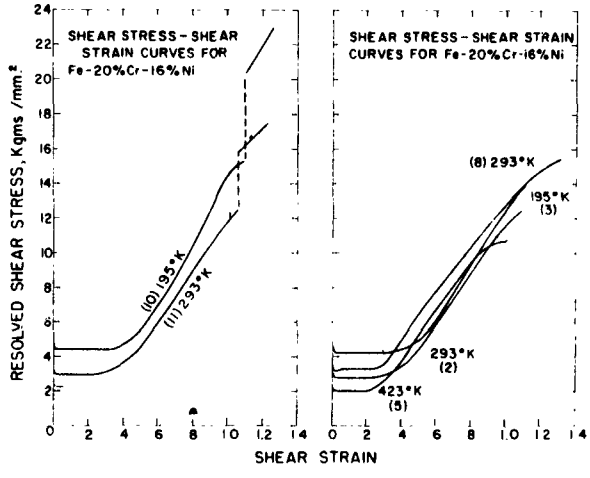

FIG. 8. Specimens of 20% Cr - 16% Ni extended at various temperatures. Figure in parentheses before temperature indicates orientation. (see Fig. 9).

77°K under zero load. Portions of several load-elongation curves are shown in Fig. 10 where various values of the resolved shear stress are indicated. It is clear that a marked variation in behaviour occurs from specimen to specimen. Sample 9 gave a sharp yield point followed by elongation under fluctuating load. Here, separated clusters of slip traces were observed along the gauge length while martensite was not distinguished by optical microscopy. Sample 4 showed a remarkable resistance to plastic flow up to substantial stresses; subsequent elongation appeared to be mainly due to martensitic transformations. While this aspect was not studied further, it is apparent that the strengths of crystals of this alloy, at 77°K, are dependent on the interaction between slip and martensite[6], and thus will not be discussed further here.

20% Cr - 12% Ni - 68% Fe

Tensile deformation of these crystals was profoundly affected by two factors, namely, the amount of ferritic phase within the austenitic matrix and the presence of martensite at low temperatures. In the following, tests in which martensite was absent will be described first.

Crystals which contained appreciable quantities of ferrite showed no drop in load at yield and no elongation

at constant load. Instead, work-hardening began immediately and multiple slip occurred in the vicinity of the ferrite inclusions. As the ferrite content was reduced by high temperature annealing treatments, an initial low hardening rate became evident until, when the crystals contained little or no ferrite, sharp yield points and Lüders' extensions were obtained.

The slip patterns of the essentially ferrite-free crystals showed no particular differences for the orientations examined. The Lüders' extensions were associated with long primary slip traces. During work hardening these slip traces increased in density while a few short traces, apparently due to slip on the cross planes, were seen. Correspondingly overshoot occurred where the tensile axis rotated towards the primary slip direction and crossed the symmetry line. This slip pattern persisted until a localized burst of slip on the conjugate planes was generated causing the sample to neck down. No region of extensive cross-slip, as is usually associated with stage III in pure single crystals and observed in some orientations of the crystals, with 16% and 20% Ni, was noted with this alloy.

During cooling to 77°K the crystals were usually largely transformed to martensite. Consequently they were of high strength and low ductility. Occasionally the

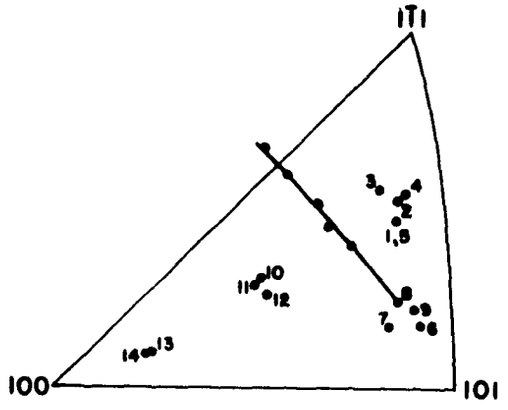

FIG. 9 Axis rotation for specimen 8, and orientations of other specimens of 20% Cr - 16% Ni used.

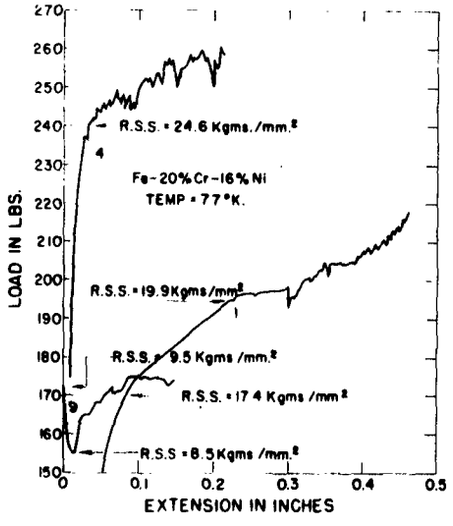

FIG 10 Some load-extension curves of 20% Cr - 16% Ni extended at 77°K showing complications due to martensite formation.

transformation was only partially completed during cooling. Elongation was then accomplished by combined slip and martensitic transformation yielding a jerky stress-strain curve.

No evidence of martensite was visible at magnifications of up to 600 times after cooling to 195°K. The response to tensile loading at this temperature was varied. Sometimes the samples showed rapid hardening accompanied by jerky flow. On these occasions martensite was present after deformation. In a few tests, the early part of the deformation apparently proceeded without any concomitant transformation. Here, in the absence of ferrite inclusions, yield was associated with a drop in load followed by a Lüders' extension. Hardening then occurred very rapidly and was accompanied by the generation of martensite.

Examples of the stress-strain curves and axial orientations are given in Figs. 11, 12 and 13.

DISCUSSION

The variation of the resolved shear stresses at yield are conveniently considered by reference to Fig. 14, in which they are plotted as functions of temperature and composition. The temperature scale is staggered for each composition to allow the points to be separated. Each stress

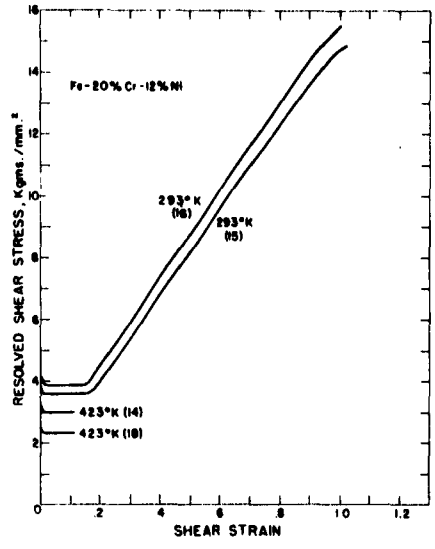

FIG. 11 Specimens of ferrite-free 20% Cr - 12% Ni extended at 293°K and 423°K.

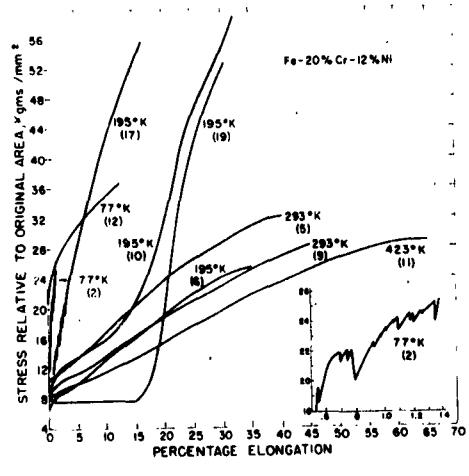

FIG. 12 Stress-elongation curves for various specimens of 20% Cr - 12% Ni showing effects of martensite formation (2, 10, 12, 17, 19) and presence of δ - ferrite (5, 6, 9, 11). For orientations, see Fig. 13.

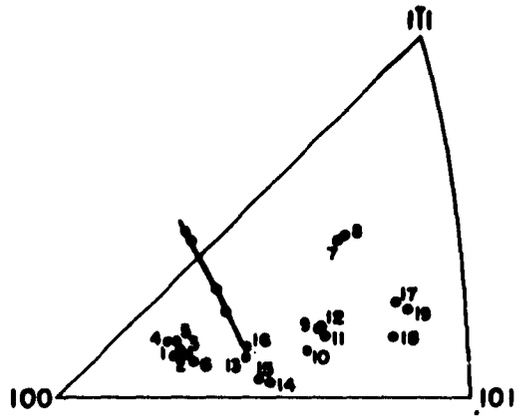

FIG. 13 Orientations of specimens of 20% Cr - 20% Ni. Axis rotation for specimen 16 is shown.

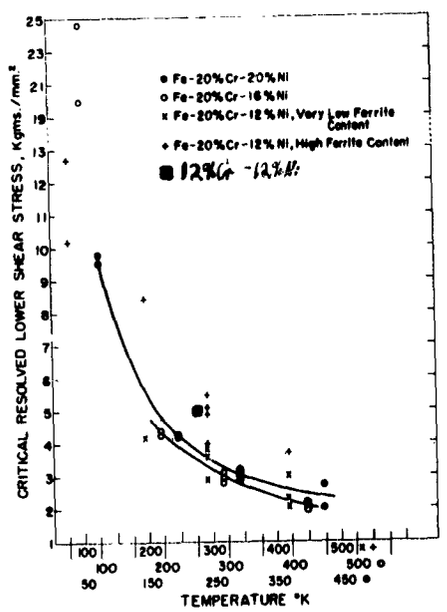

FIG. 14 Critical resolved shear stress for the various compositions as a function of test temperature. Also shown is a value for 12% Cr - 12% Ni from ref.(7).

is the lower yield point or, in the absence of a sharp yield, the apparent or true critical resolved shear stress according to whether or not yield was associated with martensitic transformations.

Data for the Fe - 20% Cr - 20% Ni alloy are the least complicated and show an increase in strength at low temperatures which is unusually large for face centred cubic alloys (see Fig. 15). The dependence of the yield stress on temperature decreased as the temperature was raised but was still significant at 423°K. For the lower nickel alloys the effects of martensite confuse the data below room temperature. At 77°K the critical resolved shear stress has little real meaning; several specimens of 16% Ni supported remarkably large stresses before deforming appreciably. The scatter in the data for the 12% Ni samples is largely due to variations in the amount and distribution of second phase within the austenitic matrix. As the ferrite content decreased the yield stresses were reduced. Apart from the effects of a second phase it is evident that no significant differences in the yield stresses of stainless steel single crystals arise when the nickel content is varied from 12% to 20%.

A single point for the c.r.s.s. of a 12% Cr - 12% Ni single crystal from the work of Salmutter and Stangler[7] is shown. The relatively high value suggests that the crystals may have contained some δ -ferrite.

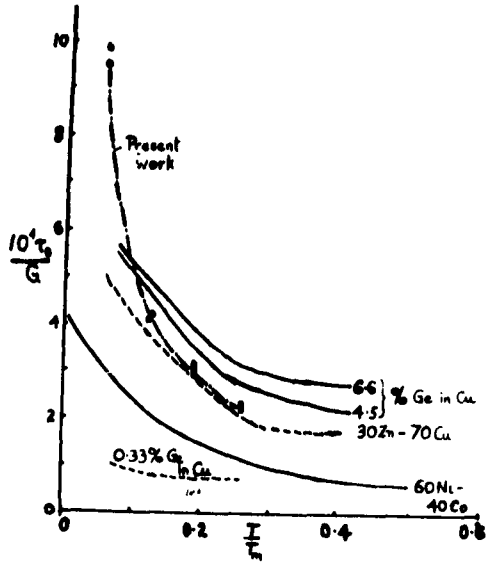

FIG. 15. Values of normalized c.r.s.s. for a variety of f.c.c. alloys as a function of homologous temperature.

For the crystals of these materials, which are free from second phase (either δ -ferrite formed during growth, or martensitic α produced by cooling and/or straining) the general shapes of the shear stress - shear strain curves (τ - ε) are also quite similar to one another. They are strongly reminiscent of the curves obtained by Ardley and Cottrell[13] and Piercy, Cahn and Cottrell[12] for 30% Zn α-brass, and for various copper base alloys by Mitchell and Hirsch[14], Brindley, Corderoy and Honeycombe[9] and Koppenaal and Fine[20], in that they show a pronounced Luders-type extension instead of the stage of easy glide (Stage I) which is characteristic of pure metals and some alloys. The present crystals also show a well defined upper and lower yield stress, as do Cu - 20% Zn and Cu - 10% In [9]. The length of easy glide or the Luder's extension is a complex function of orientation[9] , system, composition within a given system[9,12,13,14] and temperature so that further discussion does not seem warranted without more systematic data. The variation of nickel content from 12 to 20%, and temperature from 77°K to 423°K, causes variations in Luder's strain which are not significantly different in magnitude from those reported for Cu - Zn.

The curves differ in the early stages of deformation from those of other alloy crystals[8,10,16,17,20]

where the stage I or easy glide (characteristic of pure metal single crystals) is pronounced. The system which at first sight should be most similar to the present crystals is Co - Ni, which has been extensively examined by Meissner[15], Pfaff[16], Mader, Seeger and Thieringer[17] and Pfeiffer and Seeger[8]. Here the stacking fault energy varies with composition and becomes very low near 70% cobalt, above which composition the hexagonal close-packed phase becomes stable. The stacking fault energy of stainless steel is thought to vary also over the range of compositions studied here although no direct values are available. It is believed to be quite low ($\sim$13 ergs/cm^2) for 18% Cr - 8% Ni and to be greater than about 25 ergs/cm^2 for 20% Cr - 20% Ni. The derived elastic constants of Co - Ni alloys[16] are very similar to those measured by Salmutter and Stangler[7] for 12% Cr - 12% Ni austenite single crystals. These latter values have been used as an approximation in the present experiments.

In the work on Ni - Co alloys, and on Cu base alloys, stage II of work hardening terminates, i.e. stage III begins when the stress (assisted by thermal fluctuations) becomes high enough to cause cross slip. This was not always the case here. Cross-slip was observed in the A orientation for 20% Cr - 20% Ni and in crystals 2, 3, 5 and 8

of 20% Cr - 16% Ni. The tensile axes of these crystals are all well removed from [100] and the [100] [111] symmetry line. On the other hand, crystals of B orientation of 20% Cr - 20% Ni, 10 and 11 of 20% Cr - 16% Ni and the 20% Cr - 12% Ni crystals all show slip on the conjugate system when stage II ends. The axes of these crystals are all much closer to [100]. The analysis of work hardening by Seeger and his school[17] must thus be applied with some caution since this postulates thermally activated cross-slip in stage III. The values of τ_{III}/G_3† the modulus-corrected stress for the end of stage II are shown in Fig. 16. There are inadequate data to estimate the stacking fault energy from the slope of these curves, although the temperature dependence of τ_{III}/G_3 seems to be of the right order of magnitude for the stacking fault energy expected if one assumes the formulae of Seeger, Berner and Wolf[18] to apply for the specimens where cross-slip was observed.

Hardening in stage II is linear within experimental error and it is possible to make quite accurate measurements of the slope $\frac{\partial \tau}{\partial \varepsilon} = \theta_{II}$. The values of θ_{II} for all the crystals where this measurement was possible are plotted in Fig. 17 after normalizing by division by the appropriate modulus

$$G_2 = \frac{C_{44}(C_{11} - C_{12})}{2}$$

While the results, with one exception, are not

† $G_3 = \frac{C_{11} - C_{12} + C_{44}}{3}$

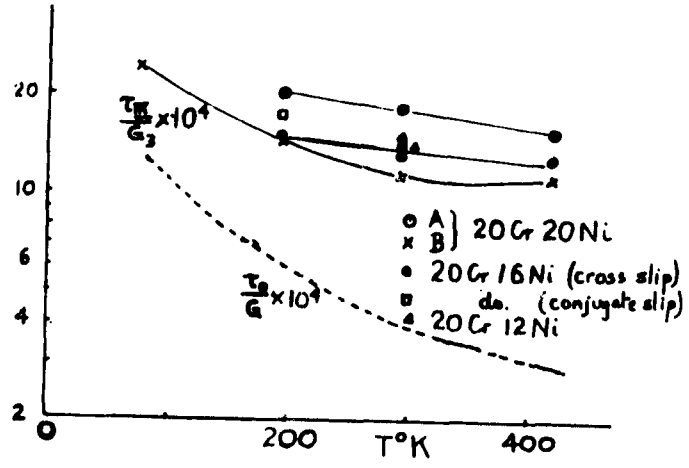

FIG. 16 Values of $3\tau_{III}/(C_{11} - C_{12} + C_{44})$ for crystals of various compositions as a function of testing

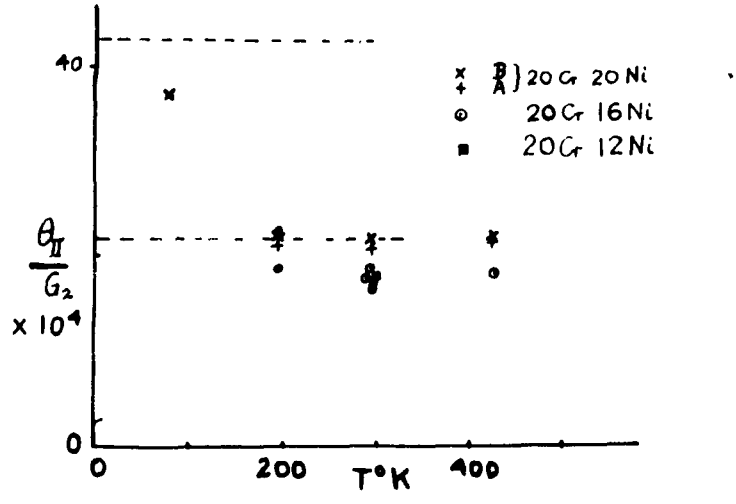

FIG. 17 Slopes of stage II of the work-hardening curves for various compositions. The band for other f.c.c. pure metals and alloys is shown[16].

temperature dependent, the absolute values are low by comparison with other f.c.c. metals and alloys[16]. The single value for 20% Cr - 20% Ni at 77°K is more nearly in line with other metals - no reason can be given for this. No evidence of martensite formation was found in this specimen. More experiments at 77°K would be advisable, but must be limited to nickel compositions greater than 16% to avoid martensite formation.

During stage II slip continued predominantly upon the primary slip system. Whether or not this stage was followed by either cross slip or slip on the conjugate system, appeared to depend upon both orientation and composition. While further systematic work is required to clarify this, it may be pointed out that for samples of group B of the 20% Ni composition the axial orientation crossed the symmetry line near the beginning of stage II so that during work hardening the applied shear stress resolved on the conjugate system exceeded and increased more rapidly than that on the operative primary system. For specimens of group A the stresses resolved on the two systems were of similar magnitude near the end of stage II. It was noteworthy that the asterism of Laue spots increased significantly after the axis crossing.

Several interesting experiments suggest themselves

from the present work. While the crystals show many points of similarity with those of other alloys, there are some differences, notably in the high temperature dependence of the initial yield and the low value of θ_{II}. Further, τ_{III} does not always correspond to the beginning of cross slip. Thus investigations using temperature-changes and strain-rate changes, together with thin film and surface replica microscopy, seem to be in order to further our knowledge of the complicated dislocation movements involved in plastic flow.

The experiments themselves suggest little difference between the various compositions which could be responsible for the known differences in stress-corrosion behaviour. It appears that experiments at substantially higher strain rates, either testing directly or by measuring resistance to propagation of a running crack[19] could be fruitful. Since carbon and nitrogen are known to have opposite effects on stress corrosion behaviour in these materials, the effects of these on mechanical properties at high strain rates should also be of interest.

CONCLUSIONS

When pulled in tension, austenitic stainless steel single crystals exhibit sharp yield points followed by Lüders' extensions of up to 20%, similar to crystals of α-brass. With no second phase present the critical resolved shear stress

is strongly temperature dependent, increasing by a factor of about 4 between 423°K and 77°K. The Lüders' extension was followed by a temperature independent low rate of linear work hardening. Unlike pure metals where profuse cross slip usually occurs at the end of linear hardening, this stage was terminated either by cross slip or by slip on the conjugate system. While the data can only be regarded as preliminary the choice between these modes appears to be dependent on both orientation and composition. No new conclusions can be drawn from the tensile deformation characteristics which may aid the understanding of stress corrosion cracking of these alloys.

ACKNOWLEDGEMENTS

This work was sponsored by the Office of Naval Research. Thanks are due to Dr. A. J. Lena of Allegheny Ludlum Steel Corporation for assistance with materials and analysis, and to W. Poling for laboratory assistance.

REFERENCES

1. C. Edeleanu. "Stress Corrosion Cracking and Embrittlement". (J. Wiley, New York 1956) p. 126.
2. H. R. Copson. "Physical Metallurgy of Stress Corrosion Fracture". (Interscience, New York 1959) p. 247.
3. R. E. Reed and H. W. Paxton. "First International Congress on Corrosion". Butterworths, London 1962.
4. R. D. Leggett, R. E. Reed and H. W. Paxton. Trans. A.I.M.E. (1959) 215, 679.
5. E. Schmid and W. Boas. "Kristallplastizitat". Springer-Verlag, Berlin 1935.
6. J. F. Breedis and W. D. Robertson. Acta Met. (in press).
7. K. Salmutter and F. Stangler. Z. fur Metallkunde (1960) 51, 544.
8. W. Pfeiffer and A. Seeger. Physica stat. solidi (1962) 2, 668.
9. B. J. Brindley, D. J. H. Corderoy and R. W. K. Honeycombe. Acta Met. (1962) 10, 1043.
10. P. Haasen and A. King. Z. fur Metallkunde (1960) 51, 722.
11. H. Suzuki. "Dislocations and Mechanical Properties of Crystals". (John Wiley, New York 1957) p. 361.
12. G. R. Piercy, R. W. Cahn and A. H. Cottrell. Acta Met. (1955) 3, 331.
13. G. W. Ardley and A. H. Cottrell. Proc. Roy. Soc. (1953) A219, 328.
14. T. E. Mitchell. Ph.D. thesis. University of Cambridge 1963.
15. J. Meissner. Z. Metallkunde (1959) 50, 207.

16. F. Pfaff. Z. Metallkunde (1962) 53, 411, 466.

17. S. Mader, A. Seeger and H. M. Thieringer. "Relation between Structure and Properties". H.M.S.O. London, 1963.

18. A. Seeger, R. Berner and H. Wolf. Z. Physik (1959) 155, 247.

19. G. Meyrick and H. W. Paxton. Unpublished work.

20. T. J. Koppenaal and M. E. Fine. Trans. A.I.M.E. (1961) 221, 1178, (1962) 224, 347.